Available online at www.sciencedirect.com
ScienceDirect
Journal of Molecular Catalysis A: Chemical 273 (2007) 81–86
JOURNAL OF MOLECULAR CATALYSIS A: CHEMICAL
www.elsevier.com/locate/molcata

One-step production of methoxymethyl benzene in electrochemical reaction of toluene with methanol assisted by modified $(NH_4)_3H_4[P(Mo_2O_7)_6]$ catalysts

Fengtao Chen, Hongzhu Ma*, Bo Wang, Qiongfang Zhuo

Institute of Energy-Chemistry, College of Chemistry and Materials Science, Shaanxi Normal University, 710062 Xi'an, PR China

Received 28 February 2007; received in revised form 26 March 2007; accepted 26 March 2007
Available online 31 March 2007

Abstract

A series of novel catalysts that P, Mo metal-salt (M_xO_y–MoO_3–P_2O_5, M = Fe, Ni, Cu) were prepared and investigated by means of TGA–DSC, XRD and XPS for elemental mapping. All catalysts exhibited good catalytic activity in the reaction of toluene with methanol, assisted with a pair of porous graphite plane electrodes, and chemical conversion higher than 92% was observed. In particular, iron promoted catalysts exhibited excellent catalytic activity. According to the experimental results, a possible free-radicals reaction mechanism confirmed by XPS and UV–vis spectra was proposed.

Keywords: Electrochemical catalytic oxidation; Toluene; Methanol; Metal-salt

1. Introduction

Oxidation of organic compounds in the liquid phase was the basis of several industrial processes developed in the past 50 years [1]. As a clean and convenient method for the generation on a preparative scale of many reactive intermediates (radical-ions, radicals, carbanions, carbocations, quinodimethanes), electrochemistry became one of the highlights in the organic synthesis and industrial chemistry [2–4]. Electrochemical synthesis in microreactors provides an attractive approach to organic synthesis and electrochemical technology, avoiding toxic, expensive organic solvents, and often providing unique pathways to control the reactant and product distribution [5,6], have received considerable attention in recent years, because of its potential applications in the synthesis of pharmaceutical drugs, amino acids, dyestuffs, pesticides, spicery and organic reagents [4,7].

Toluene is the most important aromatic hydrocarbon chemical raw material, its selective oxidation with air to synthesize benzaldehyde and benzyl alcohol, which is versatile intermediates in the chemical industry have attracted much interested [4,7–9]. But most studies on toluene were used in alkylation synthesis of *p*-xylene and its derivatives were prepared by chemical process in the presence of ZSM-5 type zeolites catalyst [7]. Benzaldehyde was synthesized from toluene using Pt–Ti alloy as the electrode in the mixture of $H_2Ce(ClO_4)_6$ and $HClO_4$ [8]. Side-chain oxidation of alkyl benzene was carried out in the medium of $Mn_2(SO_4)_3/MnSO_4$, using Pb metal as the electrode [9]. Erephthalic acid was obtained by electrolyses of *p*-xylene, *p*-methoxybenzaldehyde and *p*-cymene in $Na_2Cr_2O_7/Cr_2O_3$–50% H_2SO_4 and $Pb(H_3PO_4)$ electrode [10]. However, no much attention has been paid on the electrochemical catalytic oxidation, acylations or esterification researches at room temperature and atmospheric pressure.

In our previous work, we reported the electrochemical catalytic reaction of toluene with methanol assisted by different metals modified solid superacid catalysts [11]. Here, we report the synthesis of a series of novel catalysts derived from P, Mo metal-salt (M_xO_y–MoO_3–P_2O_5, M = Fe, Ni, Cu) and its high catalytic properties in selective oxidation of toluene to methoxymethyl benzene in methanol assisted by clean electrochemical method. The catalysts were checked by means of thermogravimetric analysis–differential scanning calorimetry (TGA–DSC), powder X-ray diffraction (XRD) and X-ray photoelectron spectroscopy (XPS) and the products were detected by

* Corresponding author. Tel.: +86 29 85308442; fax: +86 29 85307774.
E-mail address: hzmachem@snnu.edu.cn (H. Ma).

1381-1169/$ – see front matter © 2007 Elsevier B.V. All rights reserved.
doi:10.1016/j.molcata.2007.03.070

the ultraviolet–visible (UV–vis) spectrum and gas chromatography/mass spectrometry (GC/MS), the effect of the various catalysts were also discussed.

2. Experimental

2.1. Materials and general methods

All chemicals used in the experiment were analytically pure reagents and used without further purification.

The effect of the various catalysts was inspected by UV–Vis 7504 spectrum apparatus which made in Shanghai Xinmao Co., China. The component and its distribution of the products distillation were analyzed by GC /MS (QP2010, Japan). The catalyst was detected by TGA–DSC (Q600SDT American), XRD (Rigaluc, Japan) and XPS (Perkin Elmer PHI-5400).

2.2. Preparation of catalysts

$CuO–MoO_3–P_2O_5$ was prepared as follows: $Cu(NO_3)_2 \cdot 3H_2O$ and $(NH_4)_3H_4[P(Mo_2O_7)_6] \cdot 0.5H_2O$ were mixed in relevant proportions. After careful grinding, the mixture was put into a crucible and heated under the atmospheric pressure at 300 °C for 6 h. This treatment resulted in decomposition of ammonium molybdophosphate and copper nitrate. After cooling, grinding this mixture obtain the homogeneous composition. Then, this compound was allowed to react at 600 °C for 4 h to obtain $CuO–MoO_3–P_2O_5$ catalyst.

$NiO–MoO_3–P_2O_5$ and $Fe_2O_3–MoO_3–P_2O_5$ were prepared as the same way.

2.3. Experimental setup

Fig. 1 shows the schematic diagram of the experimental setup for electrochemical catalytic oxidation. The experiments were conducted in a single cell of 0.25 l capacity at 30.0 V voltage and 2.2 A current intensity. The reaction cell was cooled by the cooling water in a trough to form the room temperature condition. The reaction cell was airproofed to prevent the volatilization of methanol. The anode and cathode were positioned vertically and paralleled to each other with a constant inter-gap of 1.0 cm. The anode and cathode were both the porous graphite plate (50 mm × 50 mm × 6 mm) supplied by Spring Chemical Industrial Company Limited, Shaanxi, China. Five-gram catalyst of P, Mo metal-salt and 3.0 g assisted catalyst of KF were packed around the working electrode, forming a multi-phase electrochemical oxidation packed bed. The solution was constantly stirred at 300 rpm using a magnetic stirrer in order to maintain the uniform concentration of the electrolyte solution. The electric power was supplied with regulated dc power supply, WYK302b, Xi'an, China. The current and voltage were adjustable in the range of 0–2.5 A and 0–30 V, respectively.

2.4. Electrolysis procedures

The electrolysis was carried out in cells without compartments. The anode and cathode (graphite plate) were activated by methanol solution before using. The solvent-supporting electrolyte system was formed as follows: 3.0 g KF and 50 ml toluene were added in 60 ml anhydrous methanol with P, Mo metal-salt ($M_xO_y–MoO_3–P_2O_5$, M = Fe, Ni, Cu) catalysts (5.0 g). The resulting solutions were placed in the cells and electrolyzed at a current intensity of 2.2 A (with the time prolong, the current intensity decrease to 0.8 A gradually) with stirring at room temperature. The conversion of starting material was investigated by UV–vis spectrometry. The electronic spectra of the reaction system were detected during each electrolysis and the conversion of starting material was investigated by UV–vis spectrum every 30 min as follows: transferring 0.01 ml solution by transfer-pipette accurately and diluting it to 20 ml in a volumet-

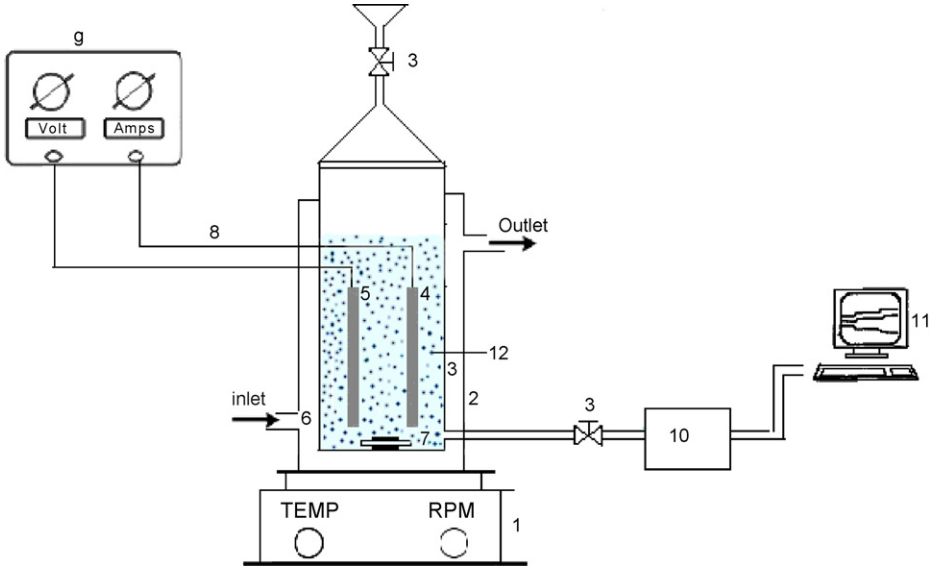

Fig. 1. Experimental setup for the electrochemical catalytic oxidation. (1) Stirring apparatus; (2) water bath; (3) electrochemical reactor; (4) graphite anode; (5) graphite cathode; (6) circulating water; (7) magnetic bar stirrer; (8) copper wire; (9) dc power; (10) distillation; (11) data acquisition and storage; (12) catalysts.

ric flask, then the electronic spectra were observed at the range of 200–400 nm using methanol as blank. The methanol used for the research of UV–vis spectrum was reclaimed for the next experiment without pollutions and waste.

2.5. Characterization of the products and the catalyst

After the reaction finished, the solution was distilled under the atmospheric pressure. The distillates were analyzed by GC/MS system using capillary column (0.25 cm × 30 m). The catalyst was washed with water for several times, dried in vacuo, then detected by XPS.

3. Results and discussion

3.1. Properties of catalyst

3.1.1. Thermal analysis

The evolutions of raw material which were copper nitrate and ammonium molybdophosphate were followed by TGA–DSC (Fig. 2). The TGA showed three weight loss steps. The first weight loss (I) appears between 30 and 151.25 °C (8 wt.%) corresponding to water desorption and coordinated water desorption. The second one (II) occurs in the range of 151–264 °C (8 wt.%), attributed to nitric acid decomposition. The last weight loss (III) appears in the range of 264–416 °C (4 wt.%), due to the decomposition of ammonium nitrate. The first broad endothermic peak observed in the range 30–216 °C corresponded to water desorption and coordinated water desorption. A modest exothermic change in the DTA curve occurs between 238 and 285 °C associated to the second TGA step. DTA peak between 394 and 448 °C was likely attributed to the decomposition of ammonium nitrate. In the range of 553.61–575 °C, an exothermic event occurred, perhaps due to the structural transition. Therefore the catalysts were calcined at 300 and 600 °C in preparation process.

3.1.2. X-ray diffraction

Fig. 3 shows the X-ray diffraction (XRD) patterns of $CuO–MoO_3–P_2O_5$ system before reaction. Compared to the PDF card of MoO_3, there are somewhat differences, which

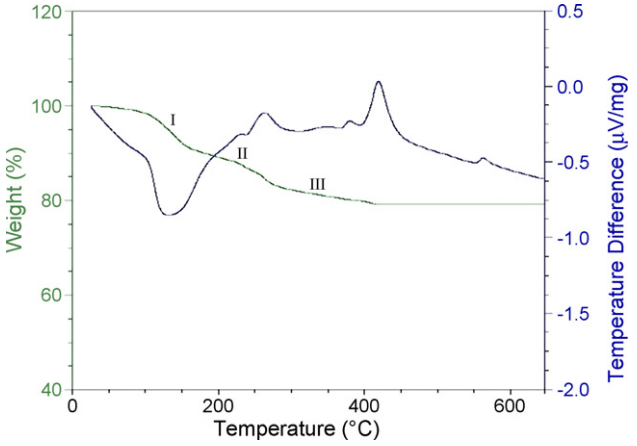

Fig. 2. TGA–DSC curves of the raw material.

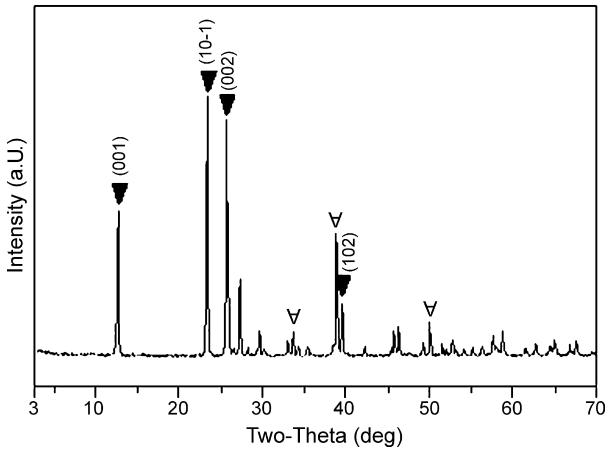

Fig. 3. XRD patterns for the $CuO–MoO_3–P_2O_5$ system before reaction.

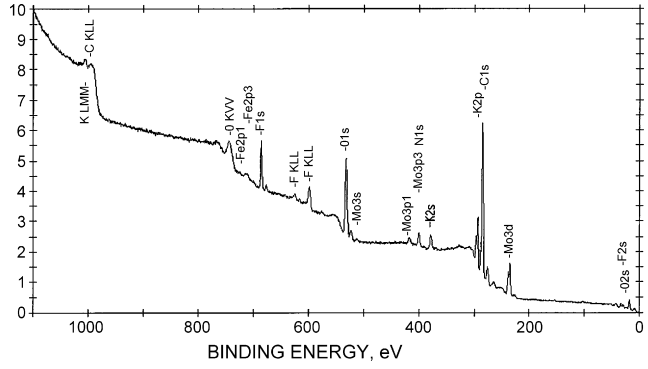

Fig. 4. The XPS survey spectra of catalyst after reaction.

perhaps due to –Mo–O– bond transformed into –O–Mo–O–, also indicating that the valence of molybdenum element in the $CuO–MoO_3–P_2O_5$ system is 6+ before reaction. Some weak diffraction patterns at $2\theta = 38.85°$, 35.398° and 49.97° can be assigned to the typical diffraction peaks of CuO–, compared to that of CuO where the representative peaks are at 38.472°, 35.244° and 48.589°, which can be explained that the location of CuO– was influenced by the $CuO–MoO_3–P_2O_5$, indicating the formation of the structure of $CuO–MoO_3–P_2O_5$.

3.1.3. XPS analysis of the catalyst after the reaction

After the coupling reaction, the $Fe_2O_3–MoO_3–P_2O_5$ catalyst was dried in vacuo and tested by XPS. The binding energy and its composition of the catalyst were shown in Fig. 4 and Table 1. XPS Fe $2p_{3/2}$ peak of the $Fe_2O_3–MoO_3–P_2O_5$ catalyst after the reaction was shown in Fig. 5.

Table 1
The components of the catalyst after the coupling reaction

Element	Area (cts/s)	Sensitivity factor	Concentration (%)
O 1s	31,832	0.711	17.07
C 1s	60,525	0.296	77.95
N 1s	2,445	0.477	1.95
P 2p	280	0.486	0.22
Mo 3d	15,003	3.321	1.72
Fe 2p	84,532	2.957	1.09

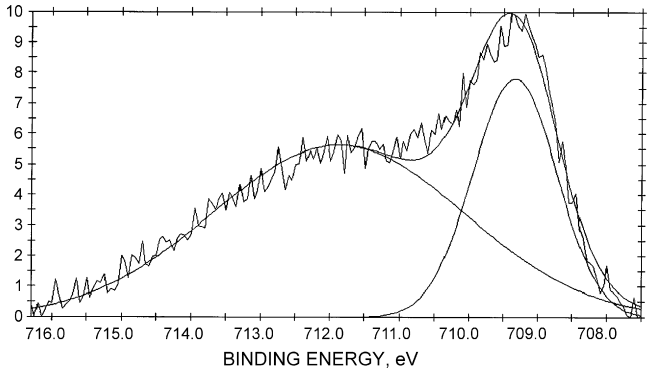

Fig. 5. The valence simulation curve of the iron in the catalyst after reaction.

The Mo 3p region of the XPS spectrum for the Fe_2O_3–MoO_3–P_2O_5 after reaction was shown in Fig. 6. In the XPS spectrum for Mo 3p, the spin–orbit components of the peak were well deconvoluted by two curves (at approximately 235.70 and 232.88 eV, respectively), which indicated that the Mo element existed mainly as the chemical state of Mo^{6+} on the basis of the principle and instrument handbook of XPS after reaction. According to the XRD pattern discussed above, the valence of Mo was 6+ before reaction, from which it can be concluded that the chemical state of molybdenum was constant during the reaction.

The XPS Fe $2p_{3/2}$ peak has been deconvoluted to two different valent components (FeO and Fe_2O_3) and the ratio of two atoms is 31.84:68.16 (molar ratio), inferred that the iron was the mixture of FeO and Fe_2O_3 in the catalyst after the reaction. Compared to that Fe^{3+} occupied 100% of the total iron element before the coupling reaction, it can illuminated that Fe^{3+} was reduced to Fe^{2+} during the coupling reaction process.

3.2. Liquid products

3.2.1. UV spectroscopy analysis

Fig. 7 shows the effect of time on the coupling reaction with Fe_2O_3–MoO_3–P_2O_5 catalyst detected by UV–vis adsorption spectrophotometer. With the time prolong (0–180 min), the K adsorption band (214 nm) of the benzene ring shifted but changed unconspicuously, and the B adsorption band of the benzene ring hypsochromic shifted from 261 to 258 nm (arrow-

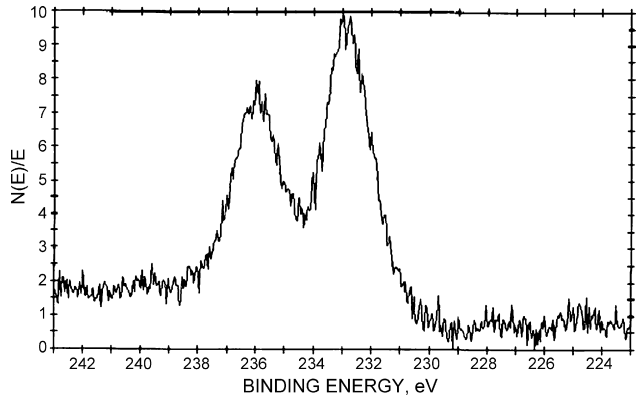

Fig. 6. The binding energy of the molybdenum in the catalyst after reaction.

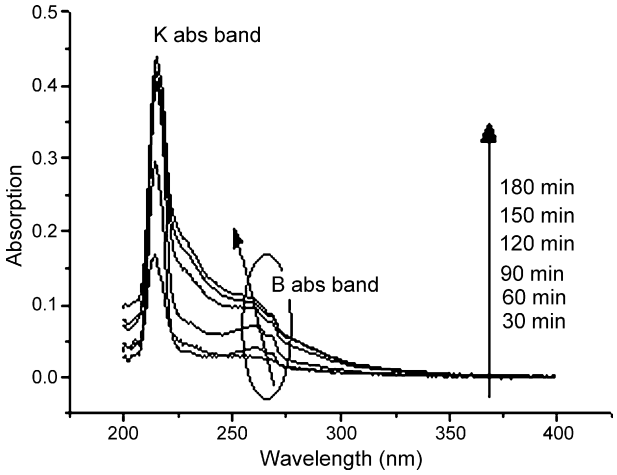

Fig. 7. The effect of time on the coupling reaction with Fe_2O_3–MoO_3–P_2O_5 as the catalyst.

head area) and the shoulder appeared from 120 min between 230 and 255 nm, owing to the interaction between the methyl of the toluene and hydroxyl group enlarged the energy band of $\pi \rightarrow \pi^*$ contrast to that of the benzene ring while hydrogen atom in the methyl of the toluene was substituted by a methoxyl group or a hydroxyl group, the conjugation between the methyl group in the toluene and the benzene ring was weakened, the energy needed by $\pi \rightarrow \pi^*$ transition increased. The increased absorption band indicated that the reaction extent was proportioned directly to the reaction time and the content of the oxygenous aromatic products.

The electronic spectra of the reaction system with $(NH_4)_3H_4[P(Mo_2O_7)_6]$ and (M_xO_y–MoO_3–P_2O_5, M = Fe, Ni, Cu) under the same reaction time of 180 min and identical current intensity of 0.8 A were shown in Fig. 8. It can be found that the K absorption band shifted unconspicuously; the adsorbed peak height of the B absorption band was decreased as follows: Fe_2O_3–MoO_3–P_2O_5 catalyst > CuO–MoO_3–P_2O_5 catalyst > NiO–MoO_3–P_2O_5 catalyst > $(NH_4)_3H_4[P(Mo_2O_7)_6]$ catalyst. This suggested that the electrochemical catalytic oxidation degree enhanced with the enhancing of catalytic activity by the different metals modification.

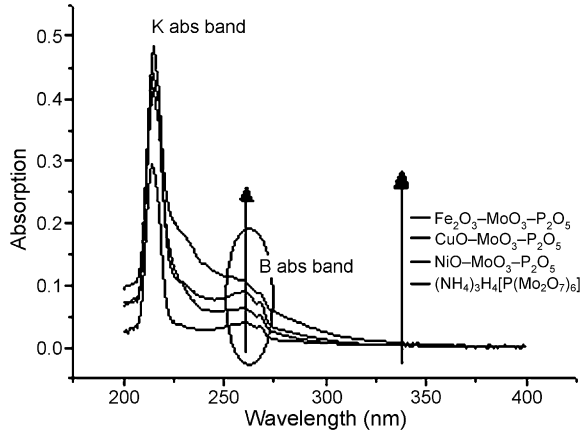

Fig. 8. The effect of the medium on the reaction system (180 min).

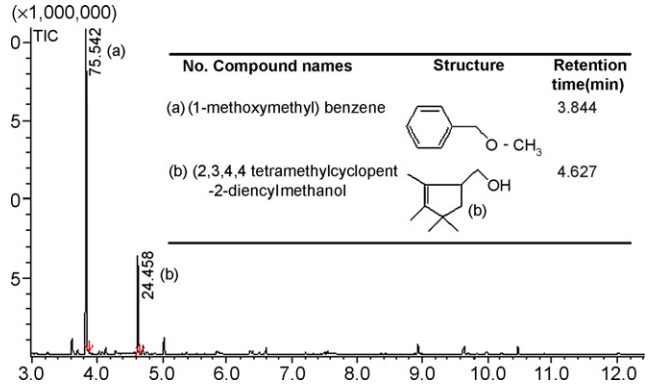

Fig. 9. The gas chromatography of the products (Fe_2O_3–MoO_3–P_2O_5 as the catalyst).

3.2.2. GC/MS spectrum

The GC of the products was shown in Fig. 9 (the peak of the solvent was taken off). Table 2 compares the percentage of the products in different mediums at the same reaction time of 180 min and the identical current intensity of 0.8 A. It can be found that the yield of the oxygenous aromatic products was higher when (M_xO_y–MoO_3–P_2O_5, M = Fe, Ni, Cu) were used than that of $(NH_4)_3H_4[P(Mo_2O_7)_6]$ catalyst; moreover, the main product 1-(methoxymethyl) benzene increased from 48.858 to 75.542%, contrasted to our previous work that the electrochemical catalytic reaction of toluene with methanol assisted by different metals modified solid superacid catalysts, the main product 1-(methoxymethyl) benzene increased from 17.455 to 51.341% [11], indicated that the catalytic activity of P, Mo metal-salt (M_xO_y–MoO_3–P_2O_5, M = Fe, Ni, Cu) catalysts is more effective than that of modified solid superacid. The highest yield was obtained with Fe_2O_3–MoO_3–P_2O_5 as catalyst in the same condition, indicated that the catalytic activities of P, Mo metal-salt catalysts were largely promoted by the addition of metals, especially with the iron element.

Table 2
The electrolysis of toluene in methanol solvent by the different catalysts[a]

Catalyst	Products concentration (mass%)[b]			Total (mass%)
	(a)	(b)	(c)	
$(NH_4)_3H_4[P(Mo_2O_7)_6]$	48.858	28.451	5.864	83.173
NiO–MoO_3–P_2O_5	57.501	25.575	5.449	88.525
CuO–MoO_3–P_2O_5	68.712	22.346	6.324	97.382
Fe_2O_3–MoO_3–P_2O_5	75.542	24.458	Little	100.00

[a] Reaction conditions: current intensity (0.8 A); reaction temperature (298 K); reaction time (180 min).

[b] GC/MS spectrum, 70 eV, M/e (relative intensity): 1-(methoxymethyl) benzene (a): 122 M^+ (50), 105 (8), 91 (100), 77 (32), 65 (24), 51 (22), 39 (22), 15 (15), 12 (2); (2,3,4,4-tetramethylcyclopent-2-dienyl)methanol (b): 154 M^+ (20), 140 (2), 139 (19), 123 (100), 105 (8), 93 (10), 81 (32), 67 (8), 41 (13), 27 (8); 1-benzyl-4-methylbenzene (c): 182 M^+ (78), 168 (13), 167 (100), 152 (25), 128 (9), 115 (10), 104 (32), 91 (15), 77 (13), 65 (14), 51 (11), 39 (13), 27 (5).

3.3. Possible mechanism

A toluene free-radical cation formed in the oxidation of side-chain of toluene assisted by P, Mo metal-salt (M_xO_y–MoO_3–P_2O_5, M = Fe, Ni, Cu) catalysts then produce a free radical. All products were obtained by the reaction of the free radical with toluene or methanol.

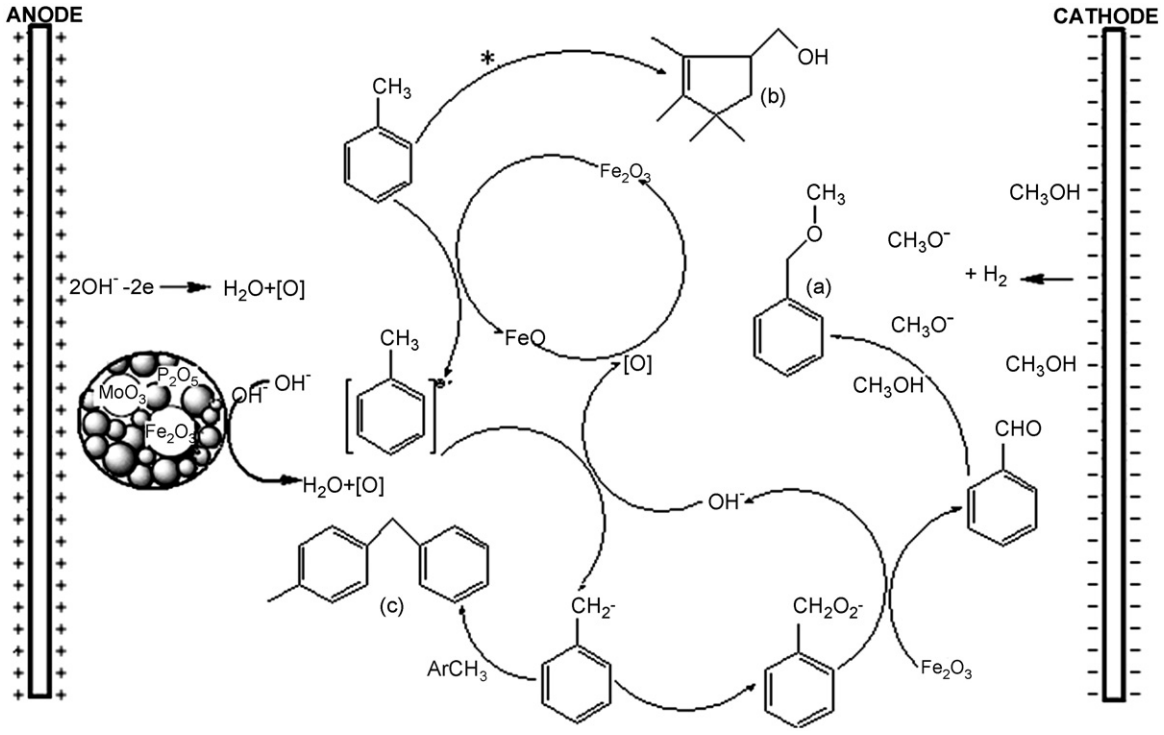

Scheme 1. The possible mechanism for the main reactions. (*) The reaction mechanisms have been unknown so far.

Oxidation proceeds via a free-radical chain mechanism, which was initiated by a change in the oxidation state of the metal, which was confirmed by XPS spectra. The benzyl radical reacted rapidly with triplet dioxygen. In the presence of a catalyst the process was ended by aromatic aldehyde formation [12,13]:

$$ArCH_3 + Fe_2O_3\text{–}MoO_3\text{–}P_2O_5 \rightarrow ArCH_2^{\bullet} + H_2O + FeO\text{–}MoO_3\text{–}P_2O_5$$

$$[ArCH_3]^{\bullet+} \rightarrow ArCH_2^{\bullet} + H^+$$

$$ArCH_2^{\bullet} + O_2 \rightarrow ArCH_2O_2^{\bullet}$$

$$ArCH_2O_2^{\bullet} + FeO\text{–}MoO_3\text{–}P_2O_5 \rightarrow ArCHO + Fe_2O_3\text{–}MoO_3\text{–}P_2O_5 + OH^-$$

The possible mechanism was proposed and listed in Scheme 1.

4. Conclusion

A novel method that electrochemical oxidation of toluene in methanol solvent catalyzed by P, Mo metal-salt (M_xO_y–MoO_3–P_2O_5, M = Fe, Ni, Cu) catalysts at room temperature and atmospheric pressure was studied. 1-(Methoxymethyl) benzene was obtained simply and effectively with high yield (92%), indicating that Fe_2O_3–MoO_3–P_2O_5 act as a good catalyst for the electrochemical reaction of toluene.

References

[1] P. Raghavendrachar, S. Ramachandran, Ind. Eng. Chem. Res. 31 (1992) 453–462.
[2] I. Nishiguchi, T. Hirashima, J. Org. Chem. 50 (1985) 539–541.
[3] H.Zh. Ma, B. Wang, Y.Q. Liang, Catal. Commun. 5 (2004) 617–620.
[4] C.J. Chang, Y. Deng, C. Shi, C.K. Chang, F.C. Anson, D.G. Nocera, Chem. Commun. 5 (2000) 1355–1359.
[5] W. Ehrfeld, V. Hessel, H. Löwe, New technology for modern chemistry, Wiley–VCH, Weinheim, Germany, 2000.
[6] A. van den Berg, W. Olthuis, P. Bergveld (Eds.), Micro Total Analysis Systems 2000: Proceedings of the TAS 2000 Symposium, Enschede, The Netherlands, May 14–18, Kluwer Academic, Boston, MA, 2000.
[7] J. Utley, Chem. Soc. Rev. 26 (1997) 157–167.
[8] K. Kramer, P.M. Robertson, N. Ibl, J. Appl. Electrochem. 10 (1980) 29–35.
[9] W. Lang, US Patent 808,075;
W. Lang, Ger. Pat. 189,178.
[10] R.M. Ergelbrecht, US Patent 3,726,914;
R.M. Ergelbrecht, US Patent 3,714,003.
[11] H.Zh. Ma, F.T. Chen, B. Wang, Q.F. Zhuo, J. Hazard. Mater. 145 (2007) 453–458.
[12] H. Vinek, Appl. Catal. 68 (1991) 277–284.
[13] J. Zhao, B. Wang, H.Z. Ma, J.T. Zhang, Ind. Eng. Chem. Res. 45 (2006) 4530–4536.